

Electrical Characterization of PEDOT:PSS Strips Deposited by Inkjet Printing on Plastic Foil for Sensor Manufacturing

Michela Borghetti, Matteo Ghittorelli, *Student Member, IEEE*, Emilio Sardini, *Member, IEEE*, Mauro Serpelloni, *Member, IEEE*, and Fabrizio Torricelli

Abstract—Inkjet printing is a viable method for rapid and low-cost manufacturing of flexible sensors. In this paper, we study a technique for inkjet printing of poly(3,4-ethylenedioxythiophene):poly(styrene sulfonate) (PEDOT:PSS) strips. A low-cost inkjet desktop printer is used for the fabrication of PEDOT:PSS resistive strips on polyimide substrates. Accounting for several geometries of printed PEDOT:PSS strips, we assess the variability of the fabrication process. Owing to the printing process, we can easily choose the width, length, and thickness. We found that printed strips on polyimide foils show a conductivity equal to 115 S/cm, which linearly increases with the strip thickness. The maximum variability is lower than 13%. The frequency analysis shows a purely resistive impedance in the frequency range investigated (100 Hz–100 kHz). Moreover, the strips folded up to 1000 times shows a resistance variation lower than 6%. The study demonstrates that inkjet printing is a viable method for the simple, fast, reliable, and low-cost fabrication of PEDOT:PSS-based sensors on plastic substrates and circuit interconnections.

Index Terms—Flexible sensors, inkjet printing, poly(3,4-ethylenedioxythiophene):poly(styrene sulfonate) (PEDOT:PSS), polymer films.

I. INTRODUCTION

CONDUCTING and semiconducting organic materials, both polymers and molecules, are opening up new application opportunities including active matrix flexible displays [1], [2], sensors [3]–[5], circuits [6], [7], wearable and implantable electronics [8]–[10], and biological and medical devices [11]–[13]. Among them, the conducting polymer poly(3,4-ethylenedioxythiophene):poly(styrene sulfonate) (PEDOT:PSS) is gaining much attention for both electronic and bioelectronic sensors. PEDOT is a π -conjugated polymer-doped p-type to a highly conducting state by PSS. A change in the doping can also be achieved by means of electrochemical doping when ions from an electrolyte enter the PEDOT:PSS film, or vice versa [14]–[18].

PEDOT:PSS shows unique feature combination compared with other conductive polymers. It is highly conductive,

air stable, available in aqueous dispersion, environmentally friendly, biocompatible, and mechanically flexible. Thanks to the aforementioned properties, PEDOT:PSS has been used for the successful fabrication of optoelectronic devices [19], [20], electronic textiles [21], [22], implantable sensors [23], physical, chemical, and biological sensors [24]–[29], and soft actuators [30]–[32].

In optoelectronic devices such as polymer thin-film transistors [19], organic light-emitting diodes [20], photovoltaic cells [33], and batteries [34], thin films of PEDOT:PSS are used as conductive electrodes and/or as interfacial layers to improve hole injection and extraction [35]. In sensors and actuators, PEDOT:PSS is patterned typically in the form of a thin strip and used as an active material in resistive elements [24], [27], [32] or electrochemical transistors [28], [29]. PEDOT:PSS is among the most widely used conducting polymers for implantable ion-pumps [9], enzyme based biosensors [12], [13], and implantable sensors [23]. Moreover, PEDOT:PSS finds relevant application as interconnections in large-area flexible circuits [36]–[38].

PEDOT:PSS can be processed from a water emulsion, at low temperature, on large area, and with low-cost deposition techniques like die coating [10] drop casting [26], [28], spin coating [24], [31], aerosol printing [39], screen printing [30], and inkjet printing [13], [40]. In particular, inkjet printing is a very appealing fabrication method because it uses a small amount of material that is directly patterned with various form factors without the need for solvents and masks. Inkjet printing is the primary choice for the inexpensive and rapid fabrication of PEDOT:PSS-based sensors on flexible, stretchable, and conformable substrates.

Inkjet-printed sensors [13], [41]–[43] have the potential to revolutionize the spread of applications. Two main challenges have to be mastered on the way toward printed sensors: 1) the development of stable sensor characteristics and 2) the development of a reliable fabrication process.

In this paper, we focus on the fabrication and characterization of inkjet printed PEDOT:PSS strips. We show the reliable fabrication of PEDOT:PSS resistive strips on polyimide foils by means of an ultralow-cost desktop inkjet printer. The combined analyses of the resistance as a function of the patterned geometries, polymer thickness, operating frequency, and stable ambient operation show that the developed fabrication process

Manuscript received February 23, 2016; revised April 16, 2016; accepted April 28, 2016. The Associate Editor coordinating the review process was Dr. Salvatore Baglio.

The authors are with the Department of Information Engineering, University of Brescia, Brescia 25123, Italy (e-mail: mauro.serpelloni@unibs.it; emilio.sardini@unibs.it).

Color versions of one or more of the figures in this paper are available online at <http://ieeexplore.ieee.org>.

Digital Object Identifier 10.1109/TIM.2016.2571518

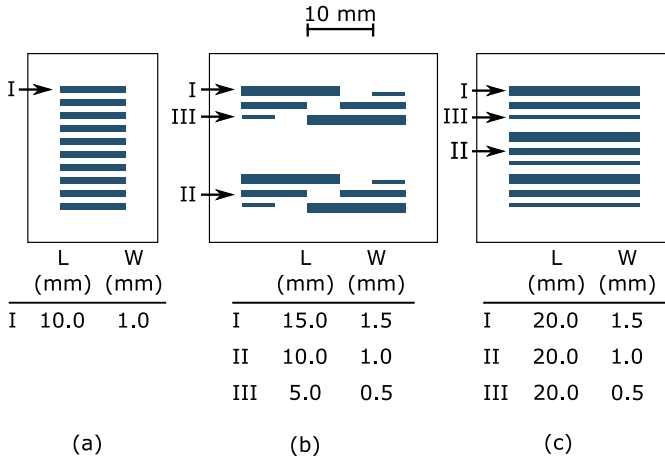


Fig. 1. PEDOT:PSS patterns used for the characterization. (a) Ten nominally identical strips. (b) Strips with nominally identical resistance but different form factors. The aspect ratio W/L is constant. (c) Strips with the same length L .

is potentially suitable for the ultralow cost, rapid, and well-controlled fabrication of a wide range of PEDOT:PSS-based sensors, biosensors, and actuators on plastic substrates. Moreover, since both the PEDOT:PSS and the polyimide substrates are biocompatible materials, the adopted technology platform is also of interest for the development of implantable sensors.

II. FABRICATION PROCESS AND MATERIALS

A. Materials

The conducting polymer PEDOT:PSS was synthesized by AGFA-Gevaert (Orgacon IJ-1005), purchased from Sigma Aldrich, and used as received. This consists of PEDOT:PSS dispersed in aqueous solution with ethanol (1%–5%) and diethylene glycol (5%–10%) [44]. The polyimide foils (Kapton HN) were purchased in 8.5 in \times 11 in sheets and with a thickness of 25 μm . The polyimide foils were cleaned and treated with oxygen plasma. Polyimide is widely used in flexible electronics as a substrate for flexible printed circuits, it is easy to clean, and it shows excellent temperature stability and radiation resistance, inherently low flammability and smoke emission, and high wear resistance. Furthermore, polyimide is biocompatible, thus enabling the use of the printed PEDOT:PSS strips in implantable devices and circuits. We used A4 paper sheets (paper density 80 g/m^2) for supporting the polyimide sample during the printing. The tape used for attaching the polyimide on the paper was Scotch Tape 2836, manufactured by 3M.

B. Fabrication

The main shape of the PEDOT:PSS strips has the following geometries: $L = 10$ mm and $W = 1$ mm, as shown in Fig. 1(a). Ten nominally identical strips were printed on the same polyimide foil. Fig. 1(b) shows the shape of several strips with the same theoretical electrical resistance but different form factors. Fig. 1(c) shows strips with the same length and several widths.

We evaluated the alignment of consecutive printings and we found that the position accuracy of the printing process

is about ± 75 μm in the horizontal direction and ± 20 μm in the vertical direction. Depending on the measurement and the form factor of the strips, the polyimide sheet was cut in 4 cm \times 4 cm foils as shown in Fig. 1. All samples were cleaned in an acetone ultrasonic bath for 15 min at room temperature. After the cleaning, the substrates were dried with air. The samples were also treated using oxygen plasma (Colibri, by Gambetti) under medium vacuum (0.5 mbar) at 35-W RF power for 180 s. The oxygen plasma etches and changes the chemical state of the polyimide surface, which becomes hydrophilic. This step is required in order to ensure the proper adhesion of the PEDOT:PSS ink on the polyimide foil. We also tried UV–ozone cleaning with different exposure times (5, 10, and 20 min), obtaining good hydrophilicity of the substrate, but we found that the adhesion of PEDOT:PSS was poor, resulting in easy peeling of the film by means of the scotch tape method. The samples were attached on the A4 paper with the tape 2836 and put on a laboratory extractor hood.

A low-cost desktop printer, Epson XP-215, was used to fabricate the PEDOT:PSS strips. The printer has four separate cartridges with 128 nozzles for black and 42 nozzles for each color. It has a maximum print resolution equal to 5760 \times 1440 dpi and the minimum droplet is 3 pl. An empty (black) cartridge was refilled with PEDOT:PSS ink. The conductive strips are printed analogously to a text document. In order to create a conductive path, the printing process must be repeated more times and at least four printing steps are needed. At each printing step, the sample was dried in a static oven for 1 min at 50 $^{\circ}\text{C}$ in order to avoid the spreading of the ink with the following printing. After depositing all layers, the sample was put in the oven for 6 min at 130 $^{\circ}\text{C}$. It is worth noting that the annealing temperature was chosen well below the boiling point of diethylene glycol (244 $^{\circ}\text{C}$) to allow the phase separation between the PEDOT and the excess PSS [14]. The phase separation enables a compact morphology, thus leading to high conductivity and stability of the printed PEDOT:PSS films. During the fabrication process, the polyimide foils were attached to an A4 paper and detached after the fabrication.

III. EXPERIMENTAL RESULTS AND DISCUSSION

The samples were measured using a Janis ST 500 cryogenic micromanipulated probe station. The probe station can operate in air or in high vacuum ($\sim 10^{-6}$ – 10^{-7} mbar). A turbo-molecular pumping station Edwards 75 was connected to the probe station chamber. The positioning of the probe tips inside the chamber was controlled using manual micrometric positioners. The probes were connected to a source meter unit Keithley 2636A, which was used for the dc electrical measurements.

A typical current–voltage (I – V) characteristic of the PEDOT:PSS strips [see Fig. 1(a), five printing steps] is shown in Fig. 2(a). Fig. 2(b) shows one portion of a strip obtained after the printing of five layers. The voltage across the strip is swept from -2 V to $+2$ V with a 100-mV voltage step in both positive and negative directions. It is worth noting that the maximum applied voltages are limited to a few volts

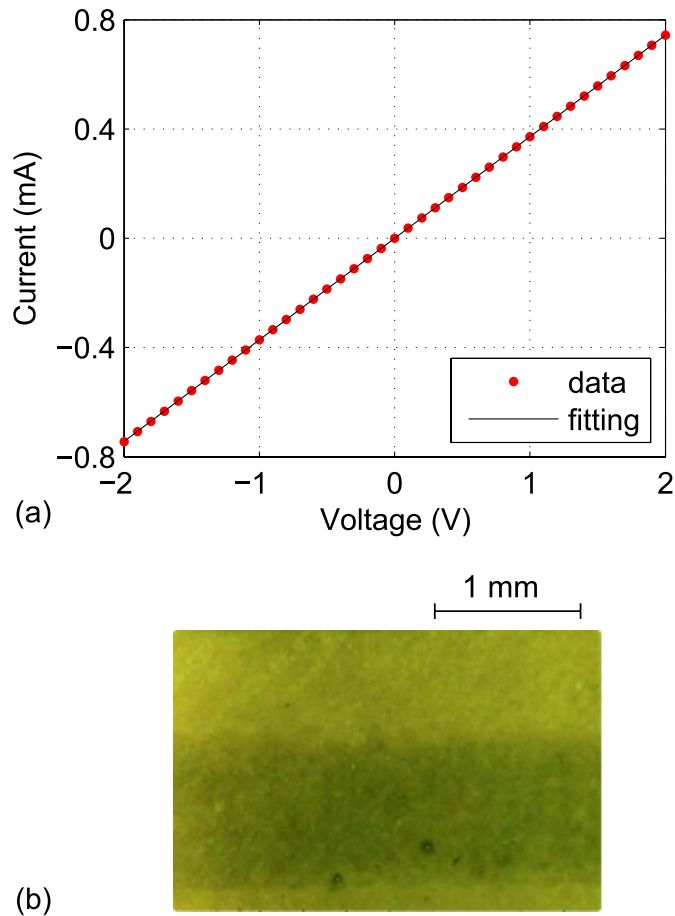


Fig. 2. (a) I - V typical characteristic of the PEDOT:PSS strips shown in Fig. 1(a) after five printing steps. (b) Photograph of a printed strip by depositing five layers of PEDOT:PSS.

in order to prevent the self-heating of the strips during the measurements [32]. Moreover, to evaluate the repeatability of the measurements, the same strip was measured three times. Symbols are the averages of the six repetitions for each voltage step and the line is the least-square approximation of $I = G \times V$, where G is the conductance of the strip. The Pearson product-moment correlation coefficient is 1 and the slope of the line is 0.37195 V/mA; the slope uncertainty is negligible. The resistance of the strip $R = 1/G$ is 2689 Ω . The maximum hysteresis is equal to 0.11%.

The I - V curve was also measured under several environmental and lighting conditions. In particular, we measured the resistance of the sample in high vacuum and in ambient (RH = 55%) under light and dark conditions. The resistance variation due to the lighting condition is negligible. Fig. 3 shows that the resistance variation due to the ambient conditions is lower than 6% with respect to the vacuum condition. The decrease in the resistance with the exposure to humidity suggests an ionic contribution to the overall conductivity [15], due to the hydration of the hydrophilic excess PSS phase of the PEDOT:PSS film [16]. However, the presence in our PEDOT:PSS of the diethylene glycol, that is, a high boiling point solvent, enables dense packing of the film, reduces the water uptake, and gives rise to a morphology less susceptible

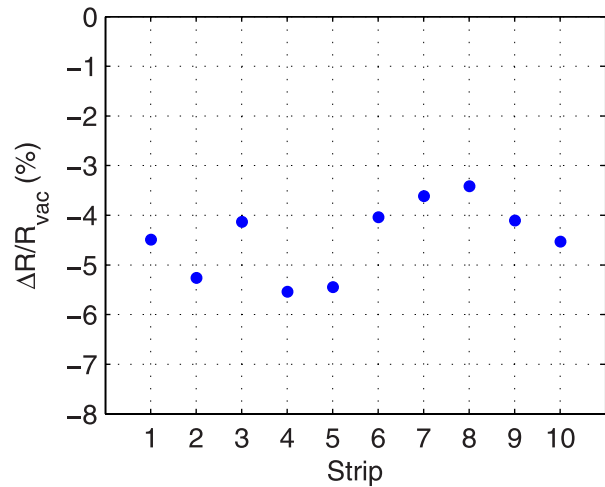


Fig. 3. Percentage resistance variation for several PEDOT:PSS strips. The strips have the same geometries: the width is 500 μm , the length is 10 mm, and the thickness is 500 nm. $\Delta R\% = 100 \times (R_{\text{amb}} - R_{\text{vac}})$, where R_{vac} and R_{amb} are the resistances measured after 48 h in vacuum and ambient (RH 55%), respectively.

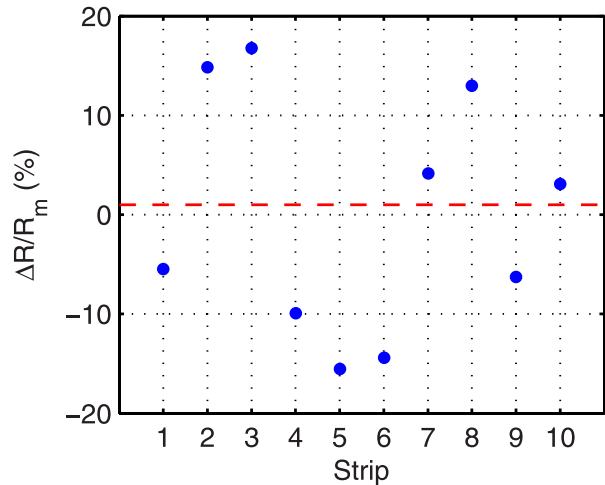
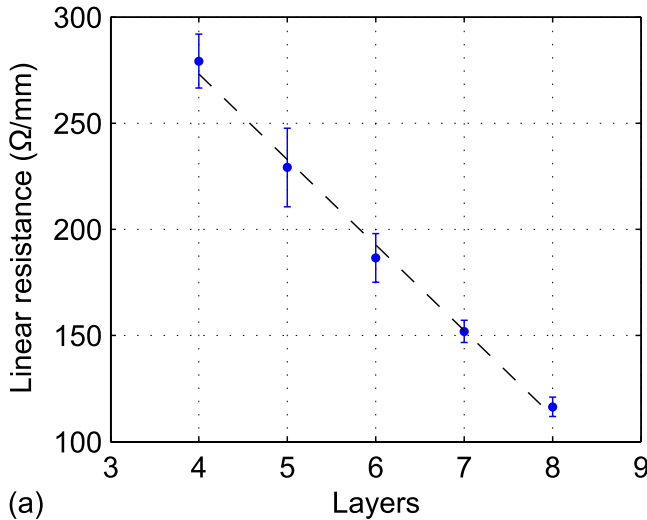


Fig. 4. Percentage resistance variation (dots) of ten nominally identical PEDOT:PSS strips [Fig. 1(a), $W = 1$ mm, $L = 10$ mm, five printing steps]. $\Delta R = 100 \times (R - R_m)$, where R is the measured resistance. The dashed line shows the average normalized resistance and it is equal to $R_m = 2.83$ k Ω .

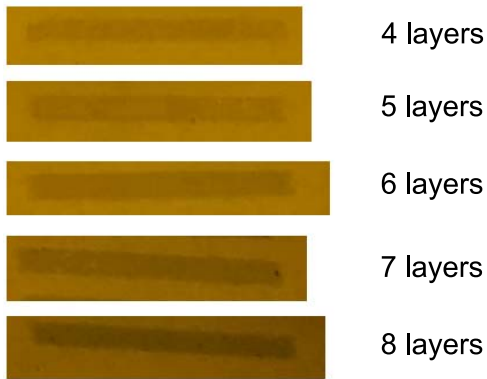
to swelling. This eventually results in a small variation of the film conductivity and thus in the measured resistances. In Fig. 4, ten nominally identical strips [the strip layout is shown in Fig. 1(a)] were measured (dots). The measurement distribution with respect to the average value (red line) results in a maximum standard deviation equal to 12%.

The relation between the resistance of the PEDOT:PSS strip and the number of printed layers is shown in Fig. 5(a). Fig. 5(b) shows the color of the strip [pattern of Fig. 1(a)] by increasing the number of printed layers. A lack of a continuous conductive layer is observed for the strips with two and three printed layers, as confirmed by the I - V measurements where the resistance of these strips is of the order of $10^9 \Omega$.

The measured resistance is proportional to the number of printings, thus suggesting that the thickness of the PEDOT:PSS strip uniformly increases with the number of printing steps. This is a crucial point for the fabrication of resistive sensors



(a)



(b)

Fig. 5. (a) Resistance measured on ten strips with the same pattern [Fig. 1(a)], varying the number of printed layers, from four to eight. The dots represent the average value of the ten nominally identical strips; the error bars represent the standard deviations. (b) Photographs of the strips as a function of the number of printed layers.

since in PEDOT:PSS, the bulk material is involved in the sensing process [24]. To further assess this point, we measured the thickness of the PEDOT:PSS strips with a stylus profilometer (Bruker Dektak XT) by varying the number of printings. The measured average thickness as a function of the number of printings is shown in Fig. 6(a). Fig. 6(c) shows the 3-D image obtained by means of a microcontact profilometer in the case of PEDOT:PSS strips after six printing steps [Fig. 6(b)]. An area of 1 mm × 0.5 mm is scanned and the film thickness shown in Fig. 6(a) is the average height. Fitting the measurements [see Fig. 6(a), dots] with a straight line, we obtained that about 101 nm of PEDOT:PSS are deposited for each printing step. Interestingly, the straight line intercepts the x -axis at $\# = 1$, which means that a single printing step does not form a continuous film. Taking advantage from the thickness characterization, we calculated the conductivity of the PEDOT:PSS film, which reads

$$\sigma = L/(WtR) \quad (1)$$

where t is thickness of the PEDOT:PSS strip. We obtained a mean value of 115 S/cm with a standard deviation of 13%. Owing to the diethylene glycol dissolved in the PEDOT:PSS,

TABLE I
SLOPE AND INTERCEPT OF THE FIRST-ORDER POLYNOMIAL
USING THE LEAST-SQUARES METHOD, VARYING THE
NUMBER OF PRINTED LAYERS

N° layers	Slope (m) (Ω/mm)	Intercept (q) (Ω)
4	273.4	88.2
5	224.9	156.1
6	175.8	205.2
7	184.8	199.0
8	110.0	139.6

the measured conductivity is two orders of magnitude higher than pure PEDOT:PSS film [40]. Diethylene glycol enables the rearrangement of the PEDOT and PSS clusters resulting in a more relaxed and compact morphology, which in turn leads to high conductivity and remarkable environmental stability [15].

A. Linearity and Contact Resistance

In order to assess the uniformity and the quality of the PEDOT:PSS film, we measured the resistance at several positions along the strip [pattern in Fig. 1(a)]. As shown in the inset of Fig. 7, we kept constant the position of one tip while changing the position the other tip with a 1-mm step. The positioning error was about 100 μ m. The relation between the resistance and the distance (d) between the two measurement points of one strip obtained with four printing steps is shown in the main panel of Fig. 7. The measurements are nicely reproduced by a straight line fitted with the least-squares approximation method. It is worth noting that a linear relation between the resistance and the distance between the tips reveals that the film conductivity and the thickness are almost constant along the PEDOT:PSS strip. We repeated this measurement on several samples by varying the PEDOT:PSS thickness (i.e., # of printing layers) in order to assess the impact of the PEDOT:PSS thickness on the linearity of the resistance. The least-square straight line fitting yields the parameters shown in Fig. 8. The slopes (m) are in good agreement with those reported in Fig. 5 and the standard deviation is always below 15%. This value is slightly higher than those obtained with the full-length devices (see Fig. 5, $L = 10$ mm) since now we have to account for both the process variability (12%) and the positioning uncertainty (10%). The extrapolation of the resistance at distance zero (q) is in the range 100–200 Ω for all the samples and thicknesses (as reported in Table I), thus revealing that the contact resistance between the gold tips and the PEDOT:PSS is not negligible. We verified that the resistance is about 150 Ω and it is independent of the thickness.

In order to further corroborate the extracted contact resistance, we performed standard four-point measurements on several strips by varying the width ($W = 0.5$ and 1 mm), length ($L = 10$ and 20 mm), and thickness ($t = 300, 500,$ and 700 nm). The width-normalized contact resistance results in $W \times R_C = 14.2 \pm 3.2 \Omega \cdot \text{cm}$. In the case $W = 1$ mm, we obtained $R_C = 142 \Omega$, which is in agreement with the length-dependent analysis shown in Figs. 7 and 8, and with the values listed in Table I.

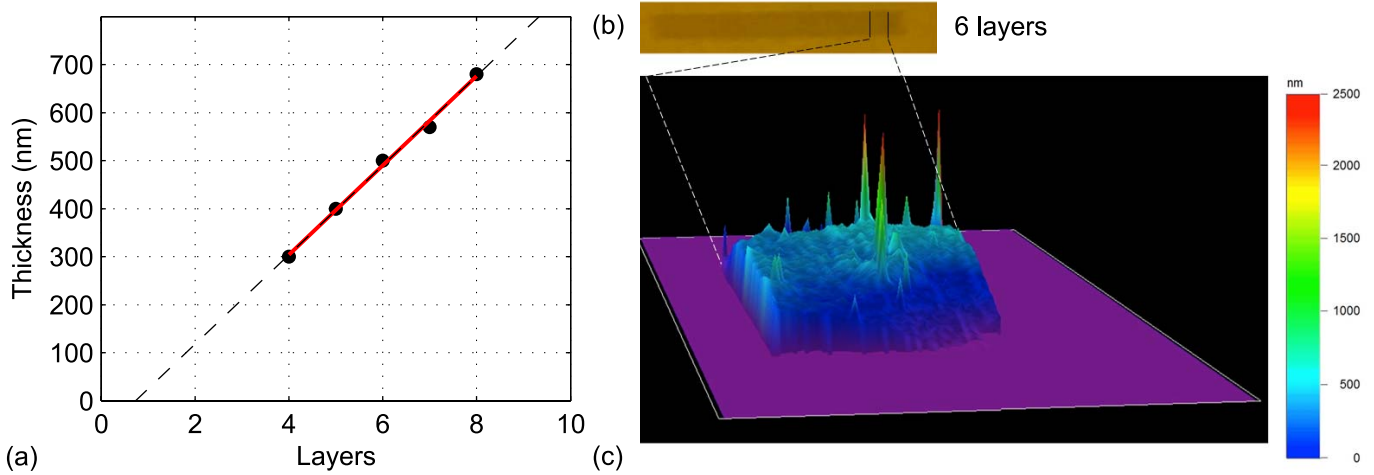


Fig. 6. Characterization of the PEDOT:PSS film thickness. (a) Measured PEDOT:PSS thickness as a function of the number of printing steps (symbols). The red line shows the last square fit with a straight line. (b) Optical image of a PEDOT:PSS strip after six printing steps. (c) 3-D image obtained by a microcontact profilometer. The scanned area is $1 \text{ mm} \times 0.5 \text{ mm}$.

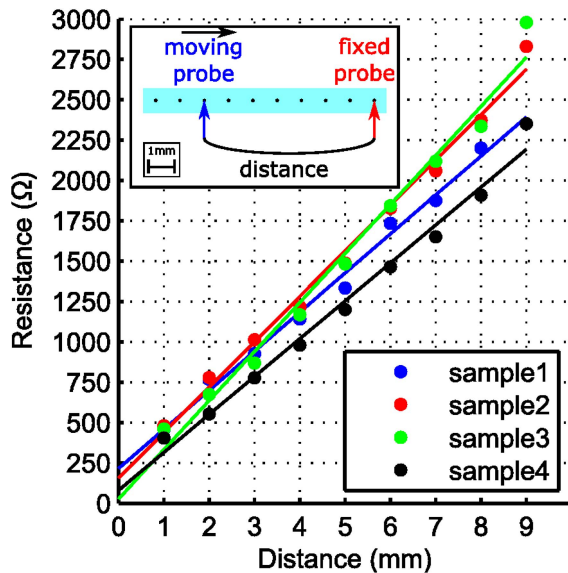


Fig. 7. Main panel: resistance as a function of the distance. Inset: measurement setup.

B. Impact of the Geometry on the Resistance

In this section, we evaluate the impact of the strip geometry on the resistance. We used the patterns shown in Fig. 1(b) where the ratio between width and length (W/L) is equal to 0.1. The number of printing steps is five. The measured resistances as a function of the strip geometry are shown in Fig. 9.

Four nominally identical strips for each geometry were measured. Since the aspect ratio (i.e., W/L) is constant, the measured resistance should be identical. The measured resistance of the geometries I and II are in agreement with those shown in Fig. 5 (five printing steps) and the variability of the four samples is below 15%. It is worth noting that in the case of geometry III, the probe positioning uncertainty is not negligible due to the small length of the strip and this results in an increased standard deviation.

In Fig. 10, the impact of the width on the resistance has been evaluated. We used the patterns shown in Fig. 1(c),

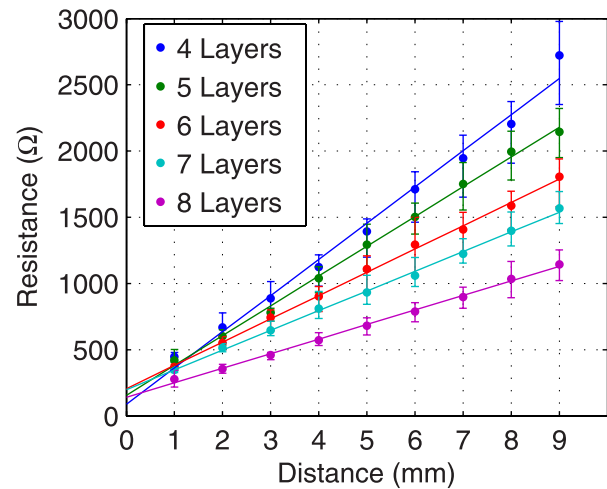


Fig. 8. Resistance as a function of the distance between the two probes. Dots are the average value of the measured resistance calculated from four samples, while the error bars represent the maximum and minimum values. The strip pattern is shown in Fig. 1(a).

where the length $L = 20 \text{ mm}$ and the widths are $W_{\text{I}} = 1.5 \text{ mm}$, $W_{\text{II}} = 1 \text{ mm}$, and $W_{\text{III}} = 0.5 \text{ mm}$. The number of printing steps is five. Four nominally identical strips for each geometry were measured. As expected, the resistance increases by decreasing the strip width [Fig. 10(a)], while the maximum variability on the four samples is about 15% [Fig. 10(b)], which is in agreement with the previous results. In order to verify the feasibility of accurate overlapping on large-scale patterns, we printed three strips with $W = 0.5 \text{ mm}$ and $L = 240 \text{ mm}$. All the printed strips show a conductivity equal to $121 \pm 2 \text{ S/cm}$. This is in agreement with the measurements shown in Figs. 5 and 6. It is worth noting that the obtained conductivity is suitable for interconnections in large-area and flexible circuits [36]–[38].

C. Frequency Characterization

In this section, we evaluate the frequency response of the printed PEDOT:PSS strips using an impedance analyzer HP4194A. All the electrical characterizations were carried

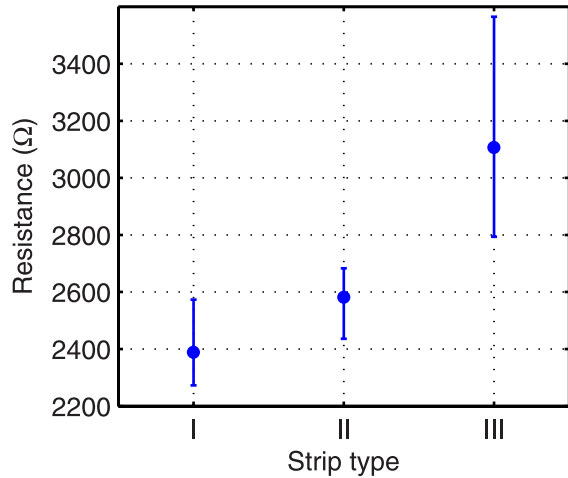


Fig. 9. Measured resistance of the strips with nominally identical resistance but several form factors [the pattern of the strips is shown in Fig. 1(b)]. The ratio between the width and the length (W/L) is 0.1. The dots represent the average value of the measured resistance calculated from four samples, while the error bars represent the maximum and minimum values.

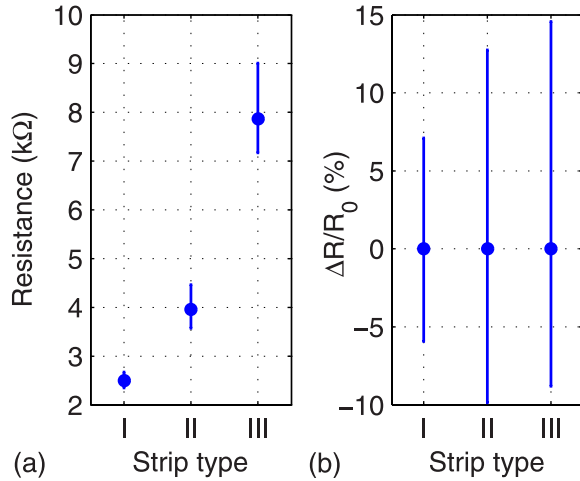


Fig. 10. (a) Impact of the width on the measured resistance [the pattern of the strips is shown in Fig. 1(c)]. The dots represent the average value of the measured resistance on four samples, while the error bars represent the maximum and minimum values. (b) Percentage resistance variation with respect to its average value R_0 . $\Delta R = 100 \times (R - R_0)$, where R is the measured resistance. The error bars represent the maximum and minimum values.

out at room temperature in ambient and light conditions. We used the patterns shown in Fig. 1(a). The number of printing steps is six. The measurements were repeated five times, showing a negligible experimental standard deviation. The average magnitude and phase of the impedance as a function of the frequency are shown in Fig. 11. The impedance is purely resistive with an about zero phase in the whole range of frequencies investigated (100 Hz–100 kHz).

D. Folding Analysis

In flexible electronics, the reliability of the fabricated devices as a function of the folding times is a crucial issue. In this section, we evaluate the folding of the printed PEDOT:PSS strips. We performed the folding test for 10, 100, and 1000 cycles. Fig. 12(a) shows the experimental setup used

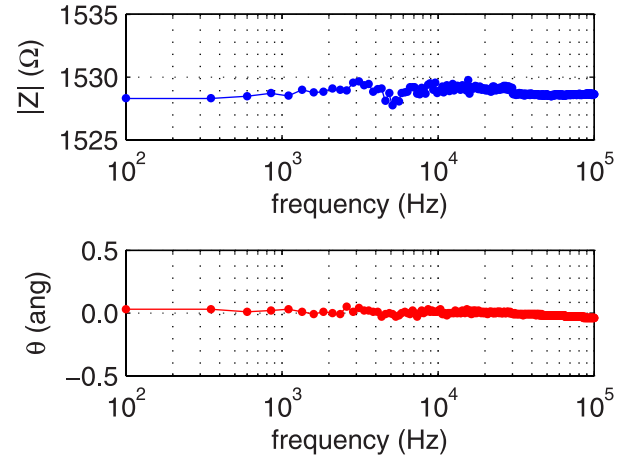


Fig. 11. Average impedance (magnitude and phase) of five measurements as a function of the frequency in the range 100 Hz–100 kHz.

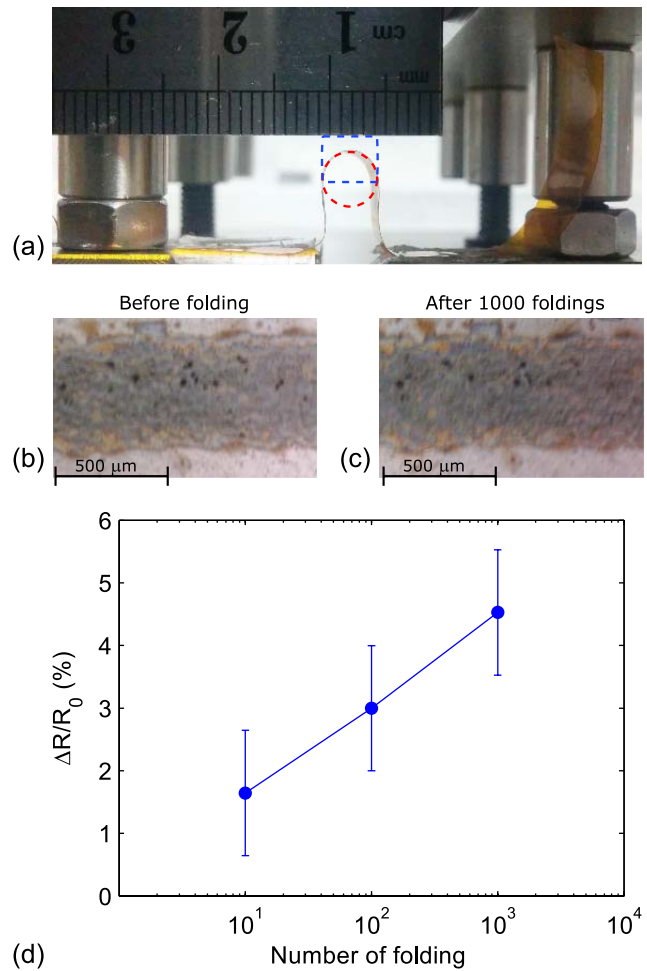


Fig. 12. (a) Experimental setup used for folding the PEDOT:PSS strips. The minimum folding radius is 2.5 mm. Optical image of the PEDOT:PSS (b) before and (c) after 1000 folding cycles. (d) Percentage resistance variation as a function of the number of folding cycles measured on six PEDOT:PSS strips, where the width is 500 μm , the length is 20 mm, and the thickness is 500 nm. $\Delta R = 100 \times (R_{N\text{fold}} - R_0)$, where $R_{N\text{fold}}$ is the resistance measured after N_{fold} folding cycles and R_0 is the resistance measured before folding. The filled circles represent the mean value and the error bars represent the maximum and minimum values.

for the folding test. The minimum curvature radius is 2.5 mm. Fig. 12(b) and (c) shows the optical image of the PEDOT:PSS film before and after 1000 folding cycles, respectively.

There is no evidence of cracks or macroscopic changes in the film morphology. This is confirmed by the relative variation of the strips resistance as a function of the folding cycles shown in Fig. 12(d). The maximum percentage variation with respect to the resistance measured before folding is lower than 6% after 1000 folding cycles.

IV. CONCLUSION

In this paper, we fabricated and characterized inkjet printed PEDOT:PSS strips. Taking advantage of an inexpensive desktop inkjet printer, we show a reliable fabrication of PEDOT:PSS resistive strips on polyimide foils. Both the substrate and the conductive polymer were selected for their biocompatible properties. The strips conductivity and the overall process variability are 115 S/cm and 13%, respectively. We fabricated strips with different aspect ratios and we evaluated the impact of the geometry on the resistance. The frequency measurements showed a purely resistive impedance in the whole range of frequencies investigated (100 Hz–100 kHz). Moreover, the strips show a resistance variation smaller than 6% if folded up to 1000 times.

The presented analysis indicates that the adopted fabrication process based on a commercially available desktop printer enables the fabrication of PEDOT:PSS resistive strips with small variability and stable electrical characteristics. These are essential features for the development of ultralow-cost inkjet-printed sensors on plastic foils.

REFERENCES

- [1] Y. Fujisaki, Y. Nakajima, T. Takei, H. Fukagawa, T. Yamamoto, and H. Fujikake, "Flexible active-matrix organic light-emitting diode display using air-stable organic semiconductor of dinaphtho[2, 3-b : 2', 3'-f]thieno[3, 2-b]-thiophene," *IEEE Trans. Electron Devices*, vol. 59, no. 12, pp. 3442–3449, Dec. 2012.
- [2] S. Abdinia *et al.*, "Organic CMOS line drivers on foil," *J. Display Technol.*, vol. 11, no. 6, pp. 564–569, 2015.
- [3] T. Xie *et al.*, "The fabrication and optimization of thin-film transistors based on poly(3-hexylthiophene) films for nitrogen dioxide detection," *IEEE Sensors J.*, vol. 16, no. 7, pp. 1865–1871, Apr. 2016.
- [4] A. Hajjam and S. Pourkamali, "Fabrication and characterization of MEMS-based resonant organic gas sensors," *IEEE Sensors J.*, vol. 12, no. 6, pp. 1958–1964, Jun. 2012.
- [5] H.-W. Zan, M.-Z. Dai, T.-Y. Hsu, H.-C. Lin, H.-F. Meng, and Y.-S. Yang, "Porous organic TFTs for the applications on real-time and sensitive gas sensors," *IEEE Electron Device Lett.*, vol. 32, no. 8, pp. 1143–1145, Aug. 2011.
- [6] A. Bozkurt and A. Lal, "Low-cost flexible printed circuit technology based microelectrode array for extracellular stimulation of the invertebrate locomotory system," *Sens. Actuators A, Phys.*, vol. 169, no. 1, pp. 89–97, Sep. 2011.
- [7] S. Abdinia *et al.*, "Variation-based design of an AM demodulator in a printed complementary organic technology," *Organic Electron.*, vol. 15, no. 4, pp. 904–912, Apr. 2014.
- [8] G. Schwartz *et al.*, "Flexible polymer transistors with high pressure sensitivity for application in electronic skin and health monitoring," *Nature Commun.*, vol. 4, May 2013, Art. no. 1859.
- [9] J. Isaksson, P. Kjäll, D. Nilsson, N. Robinson, M. Berggren, and A. Richter-Dahlfors, "Electronic control of Ca^{2+} signalling in neuronal cells using an organic electronic ion pump," *Nature Mater.*, vol. 6, no. 9, pp. 673–679, 2007.
- [10] S. Takamatsu, T. Kobayashi, N. Shibayama, K. Miyake, and T. Itoh, "Fabric pressure sensor array fabricated with die-coating and weaving techniques," *Sens. Actuators A, Phys.*, vol. 184, pp. 57–63, Sep. 2012.
- [11] K. Kuribara *et al.*, "Organic transistors with high thermal stability for medical applications," *Nature Commun.*, vol. 3, Mar. 2012, Art. no. 723.
- [12] J. Liu, M. Agarwal, and K. Varahramyan, "Glucose sensor based on organic thin film transistor using glucose oxidase and conducting polymer," *Sens. Actuators B, Chem.*, vol. 135, no. 1, pp. 195–199, 2008.
- [13] A. Phongphut, C. Sriprachubwong, A. Wisitorsaat, A. Tuantranont, S. Prichanont, and P. Sritongkham, "A disposable amperometric biosensor based on inkjet-printed Au/PEDOT-PSS nanocomposite for triglyceride determination," *Sens. Actuators B, Chem.*, vol. 178, pp. 501–507, Mar. 2013.
- [14] X. Crispin *et al.*, "The origin of the high conductivity of poly(3,4-ethylenedioxythiophene)-poly(styrenesulfonate) (PEDOT-PSS) plastic electrodes," *Chem. Mater.*, vol. 18, no. 18, pp. 4354–4360, 2006.
- [15] A. M. Nardes, M. Kemerink, M. M. de Kok, E. Vinken, K. Maturova, and R. A. J. Janssen, "Conductivity, work function, and environmental stability of PEDOT:PSS thin films treated with sorbitol," *Organic Electron.*, vol. 9, no. 5, pp. 727–734, 2008.
- [16] T. Stöcker, A. Köhler, and R. Moos, "Why does the electrical conductivity in PEDOT:PSS decrease with PSS content? A study combining thermoelectric measurements with impedance spectroscopy," *J. Polym. Sci. B, Polym. Phys.*, vol. 50, no. 14, pp. 976–983, 2012.
- [17] K. van de Ruit *et al.*, "Quasi-one dimensional in-plane conductivity in filamentary films of PEDOT:PSS," *Adv. Funct. Mater.*, vol. 23, no. 46, pp. 5778–5786, Dec. 2013.
- [18] S. van Reenen, M. Scheepers, K. van de Ruit, D. Bollen, and M. Kemerink, "Explaining the effects of processing on the electrical properties of PEDOT:PSS," *Organic Electron.*, vol. 15, no. 12, pp. 3710–3714, 2014.
- [19] J. H. Cho *et al.*, "Printable ion-gel gate dielectrics for low-voltage polymer thin-film transistors on plastic," *Nature Mater.*, vol. 7, no. 11, pp. 900–906, 2008.
- [20] H. B. Akkerman, P. W. M. Blom, D. M. de Leeuw, and B. de Boer, "Towards molecular electronics with large-area molecular junctions," *Nature*, vol. 441, no. 7089, pp. 69–72, 2006.
- [21] D. Pani, A. Dessi, J. F. Saenz-Cogollo, G. Barabino, B. Fraboni, and A. Bonfiglio, "Fully textile, PEDOT:PSS based electrodes for wearable ECG monitoring systems," *IEEE Trans. Biomed. Eng.*, vol. 63, no. 3, pp. 540–549, Mar. 2016.
- [22] S. Khumpuang, K. Miyake, and T. Itoh, "Characterization of a SWNT-reinforced conductive polymer and patterning technique for applications of electronic textile," *Sens. Actuators A, Phys.*, vol. 169, no. 2, pp. 378–382, 2011.
- [23] A. Bozkurt, R. F. Gilmour, and A. Lal, "In vivo electrochemical characterization of a tissue-electrode interface during metamorphic growth," *IEEE Trans. Biomed. Eng.*, vol. 58, no. 8, pp. 2401–2406, Aug. 2011.
- [24] G. Latessa, F. Brunetti, A. Reale, G. Saggio, and A. Di Carlo, "Piezoresistive behaviour of flexible PEDOT:PSS based sensors," *Sens. Actuators B, Chem.*, vol. 139, no. 2, pp. 304–309, 2009.
- [25] H. Tang, P. Lin, H. L. W. Chan, and F. Yan, "Highly sensitive dopamine biosensors based on organic electrochemical transistors," *Biosens. Bioelectron.*, vol. 26, no. 11, pp. 4559–4563, 2011.
- [26] S. Cruz, D. Dias, J. C. Viana, and L. A. Rocha, "Inkjet printed pressure sensing platform for postural imbalance monitoring," *IEEE Trans. Instrum. Meas.*, vol. 64, no. 10, pp. 2813–2820, Oct. 2015.
- [27] R. Faddoul, R. Coppard, and T. Berthelot, "Inkjet printing of organic electrochemical immunosensors," in *Proc. IEEE SENSORS*, Nov. 2014, pp. 1088–1091.
- [28] Z. Wang *et al.*, "Facile preparation of highly water-stable and flexible PEDOT:PSS organic/inorganic composite materials and their application in electrochemical sensors," *Sens. Actuators B, Chem.*, vol. 196, pp. 357–369, Jun. 2014.
- [29] M. Wagner, G. Lisak, A. Ivaska, and J. Bobacka, "Durable PEDOT:PSS films obtained from modified water-based inks for electrochemical sensors," *Sens. Actuators B, Chem.*, vol. 181, pp. 694–701, May 2013.
- [30] K. Ren, S. Liu, M. Lin, Y. Wang, and Q. M. Zhang, "A compact electroactive polymer actuator suitable for refreshable Braille display," *Sens. Actuators A, Phys.*, vol. 143, no. 2, pp. 335–342, 2008.
- [31] G. Ouyang, K. Wang, L. Henriksen, M. N. Akram, and X. Y. Chen, "A novel tunable grating fabricated with viscoelastic polymer (PDMS) and conductive polymer (PEDOT)," *Sens. Actuators A, Phys.*, vol. 158, no. 2, pp. 313–319, 2010.
- [32] S. Taccola, F. Greco, E. Sinibaldi, A. Mondini, B. Mazzolai, and V. Mattoli, "Toward a new generation of electrically controllable hygro-morphic soft actuators," *Adv. Mater.*, vol. 27, no. 10, pp. 1668–1675, Jan. 2015.
- [33] J.-W. Kang *et al.*, "Fully spray-coated inverted organic solar cells," *Solar Energy Mater. Solar Cells*, vol. 103, pp. 76–79, Aug. 2012.

- [34] Y. Xuan, M. Sandberg, M. Berggren, and X. Crispin, "An all-polymer-air PEDOT battery," *Organic Electron.*, vol. 13, no. 4, pp. 632–637, 2012.
- [35] J. J. Brondijk, F. Torricelli, E. C. P. Smits, P. W. M. Blom, and D. M. de Leeuw, "Gate-bias assisted charge injection in organic field-effect transistors," *Organic Electron.*, vol. 13, no. 9, pp. 1526–1531, 2012.
- [36] F. J. Touwslager, N. P. Willard, and D. M. de Leeuw, "I-line lithography of poly-(3,4-ethylenedioxythiophene) electrodes and application in all-polymer integrated circuits," *Appl. Phys. Lett.*, vol. 81, no. 24, pp. 4556–4558, Dec. 2002.
- [37] H. Siringhaus *et al.*, "High-resolution inkjet printing of all-polymer transistor circuits," *Science*, vol. 290, no. 5499, pp. 2123–2126, Dec. 2000.
- [38] T. Kawase, H. Siringhaus, R. H. Friend, and T. Shimoda, "Inkjet printed via-hole interconnections and resistors for all-polymer transistor circuits," *Adv. Mater.*, vol. 13, no. 21, pp. 1601–1605, Nov. 2001.
- [39] B. Thompson and H.-S. Yoon, "Aerosol-printed strain sensor using PEDOT:PSS," *IEEE Sensors J.*, vol. 13, no. 11, pp. 4256–4263, Nov. 2013.
- [40] L. Basiricò, P. Cosseddu, A. Scidà, B. Fraboni, G. G. Malliaras, and A. Bonfiglio, "Electrical characteristics of ink-jet printed, all-polymer electrochemical transistors," *Organic Electron.*, vol. 13, no. 2, pp. 244–248, 2012.
- [41] B. Andò and S. Baglio, "All-inkjet printed strain sensors," *IEEE Sensors J.*, vol. 13, no. 12, pp. 4874–4879, Dec. 2013.
- [42] B. Andò, S. Baglio, C. O. Lombardo, V. Marletta, and A. Pistorio, "A low-cost accelerometer developed by inkjet printing technology," *IEEE Trans. Instrum. Meas.*, vol. 65, no. 5, pp. 1242–1248, May 2015, accessed on Feb. 22, 2015. [Online]. Available: <http://ieeexplore.ieee.org/stamp/stamp.jsp?tp=&arnumber=7317561&isnumber=4407674>
- [43] M. Borghetti, E. Sardini, and M. Serpelloni, "Preliminary study of resistive sensors in inkjet technology for force measurements in biomedical applications," in *Proc. IEEE 11th Int. Multi-Conf. Syst., Signals Devices*, Feb. 2014, pp. 1–4.
- [44] S. Aldrich. 739316 *Aldrich Poly(3,4-Ethylenedioxythiophene)-Poly(Styrenesulfonate)*, accessed on Feb. 22, 2015. [Online]. Available: <http://www.sigmaaldrich.com/catalog/product/aldrich/739316>



Michela Borghetti received the master's (*cum laude*) degree in electronics engineering and the Ph.D. degree in technology for health from the University of Brescia, Brescia, Italy, in 2012 and 2016, respectively.

She was a Visiting Ph.D. Student with the Universitat Politècnica de Catalunya, Barcelona, Spain, in 2015. She is currently a Post-Doctoral Researcher with the Department of Information Engineering, University of Brescia. She is also involved in the design and fabrication of sensors for healthcare

using low-cost technologies. Furthermore, she is developing electronic systems for measuring and monitoring limb movements.



Matteo Ghittorelli (S'15) received the M.S. degree from the University of Brescia, Brescia, Italy, in 2012, where he is currently pursuing the Ph.D. degree.

His current research interests include the physical modeling of organic and amorphous-oxide materials, and the design of high-functionality circuits in emerging large-area technologies.



Emilio Sardini (M'99) received the Laurea degree in electronics engineering from the Polytechnic University of Milan, Milan, Italy, in 1983.

He conducts the research and teaching activities with the Department of Electronics for Automation, University of Brescia, Brescia, Italy, since 1984, where he has been a Full Professor of Electrical and Electronic Measurement since 2006. He has done intensive research in the field of electronic instrumentation, sensors, and signal conditioning electronics. He has authored or co-authored over 100 papers in international journal. His current research interests include the development of autonomous sensors for biomedical applications with some specific interest toward the devices implantable inside the human body.



Mauro Serpelloni (M'12) received the Ph.D. degree in electronic instrumentation from the University of Brescia, Brescia, Italy, in 2006.

He was a Post-Doctoral Researcher with the Department of Information Engineering, University of Brescia, from 2006 to 2010. He is currently an Assistant Professor of Measurement with the Information Engineering Department, University of Brescia. He is an Assistant Professor and Aggregate Professor with the Department of Information Engineering, University of Brescia. He has been

involved in several projects relating to the design, modeling, and fabrication of measurement systems for industrial applications. His current research interests include electronic instrumentation, sensors, contactless transmissions between sensors and electronics, and signal processing for microelectromechanical systems.



Fabrizio Torricelli received the Ph.D. degree from the University of Brescia, Brescia, Italy, in 2010.

He was a Post-Doctoral Fellow with the Eindhoven University of Technology, Eindhoven, The Netherlands, from 2010 to 2012. He is currently an Assistant Professor with the University of Brescia. His current research interests include organic and amorphous-oxide devices, the design of electronic devices in flexible and printed technologies, and the development of nonvolatile memories.